Appendix

Table 1. Blind denoising MSE results of our DIP network, Lasso in the DCT basis, sym4 wavelet denoising, and Wiener Filter on audio data. Univariate time series of a whale call, speech, and a drum beat were perturbed with AWGN with 0 mean and standard deviations 0.1,0.15, and 0.2.

Method	Whale			Speech			Beat		
	$\sigma = 0.1$	$\sigma = 0.15$	$\sigma = 0.2$	$\sigma = 0.1$	$\sigma = 0.15$	$\sigma = 0.2$	$\sigma = 0.1$	$\sigma = 0.15$	$\sigma = 0.2$
Ours	0.0038	0.0058	0.0133	0.0059	0.0094	0.0284	0.0029	0.0038	0.0043
Lasso	0.0499	0.0522	0.0584	0.0104	0.0131	0.0197	0.0062	0.0088	0.0151
Wavelet	**0.0032**	**0.0054**	**0.0075**	**0.0047**	**0.0078**	**0.0116**	**0.0008**	**0.0012**	**0.0017**
Wiener	0.0260	0.0297	0.0362	0.0138	0.0184	0.0251	0.0052	0.0096	0.0171

Table 2. Blind denoising MSE results of our DIP network, Lasso in the DCT basis, sym4 wavelet denoising, and Wiener Filter on artificial chirp signals. Univariate time series of chirps with a 500 hz, 300 hz, and 100 hz frequency shift were perturbed with AWGN with 0 mean and standard deviations 0.1,0.15, and 0.2.

Method	500 hz			300 hz			100 hz		
	$\sigma = 0.1$	$\sigma = 0.15$	$\sigma = 0.2$	$\sigma = 0.1$	$\sigma = 0.15$	$\sigma = 0.2$	$\sigma = 0.1$	$\sigma = 0.15$	$\sigma = 0.2$
Ours	0.0092	0.0109	0.0689	0.0086	0.0087	0.0290	0.0078	0.0071	0.0114
Lasso	0.0049	**0.0086**	**0.0161**	**0.0032**	**0.0062**	**0.0136**	**0.0015**	**0.0040**	**0.0106**
Wavelet	**0.0045**	0.0104	0.0189	0.0053	0.0108	0.0215	0.0060	0.0128	0.0213
Wiener	0.1693	0.1793	0.1893	0.1703	0.1788	0.1894	0.1696	0.1789	0.1882

Table 3. MSE results for reconstructing a signal from $m = 10, 25, 50, 75,$ and 150 DCT coefficient measurements of air sensor time series with $n = 1024$. We compare our DIP method to Lasso in the DCT basis, NLM-VAMP, and Wiener-VAMP. The best MSE value for each test is bolded. DNC indicates that the algorithm did not converge.

METHOD	O3				
	$m = 10$	$m = 25$	$m = 50$	$m = 75$	$m = 150$
OURS	0.2185	0.1835	0.1594	0.1519	0.1433
LASSO	**0.2063**	0.2036	**0.1578**	**0.1496**	**0.1396**
NLM-VAMP	DNC	DNC	DNC	DNC	DNC
WIENER-VAMP	DNC	DNC	DNC	DNC	0.1485
	NO2				
	$m = 10$	$m = 25$	$m = 50$	$m = 75$	$m = 150$
OURS	**0.2060**	**0.2051**	0.1594	0.1533	0.1372
LASSO	0.2062	0.2059	**0.1552**	**0.1492**	**0.1297**
NLM-VAMP	DNC	DNC	DNC	DNC	DNC
WIENER-VAMP	DNC	DNC	DNC	DNC	0.1400
	CO				
	$m = 10$	$m = 25$	$m = 50$	$m = 75$	$m = 150$
OURS	**0.2496**	**0.2474**	**0.2468**	**0.2307**	0.1161
LASSO	0.2540	0.2534	0.2522	0.2471	**0.1107**
NLM-VAMP	DNC	DNC	DNC	DNC	DNC
WIENER-VAMP	DNC	0.3126	0.2747	0.2695	DNC

Table 4. MSE results for reconstructing a signal from $m = 100, 500, 1000, 2000,$ and 4000 DCT coefficient measurements of artificial chirp signals with $n = 16,384$ and linear phase shifts of 500 hz, 300 hz, and 100 hz. We compare our DIP method to Lasso in the DCT basis, NLM-VAMP, and Wiener-VAMP. The best MSE value for each test is bolded. DNC indicates that the algorithm did not converge.

METHOD	500 HZ				
	$m = 100$	$m = 500$	$m = 1000$	$m = 2000$	$m = 4000$
OURS	0.5013	0.5003	0.4844	0.4552	0.3919
LASSO	**0.4973**	**0.4872**	**0.4676**	**0.4367**	**0.3725**
NLM-VAMP	DNC	DNC	DNC	DNC	DNC
WIENER-VAMP	DNC	DNC	0.6357	0.4625	0.4055
	300 HZ				
	$m = 100$	$m = 500$	$m = 1000$	$m = 2000$	$m = 4000$
OURS	0.4998	0.4949	0.4749	0.4506	0.4053
LASSO	**0.4972**	**0.4896**	**0.4657**	**0.4356**	**0.3812**
NLM-VAMP	DNC	DNC	DNC	DNC	DNC
WIENER-VAMP	DNC	DNC	0.6437	0.4619	0.4177
	100 HZ				
	$m = 100$	$m = 500$	$m = 1000$	$m = 2000$	$m = 4000$
OURS	0.5009	**0.4858**	**0.4517**	**0.4255**	0.3923
LASSO	**0.4959**	0.4864	0.4551	0.4261	**0.3665**
NLM-VAMP	DNC	DNC	DNC	DNC	DNC
WIENER-VAMP	DNC	DNC	DNC	0.4562	0.3997

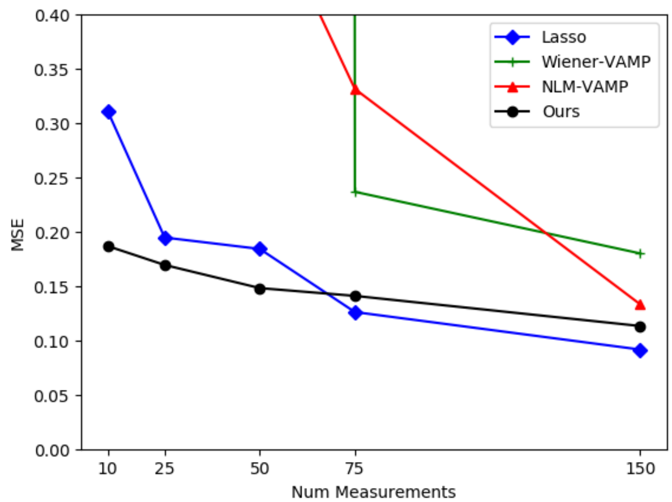

Figure 1. Test loss for recovery from random Gaussian projections on hourly sensor readings of NO2 in the air with $n = 1024$ and varying numbers of measurement by our method, Lasso in the DCT basis, NLM-VAMP, and Wiener-VAMP.

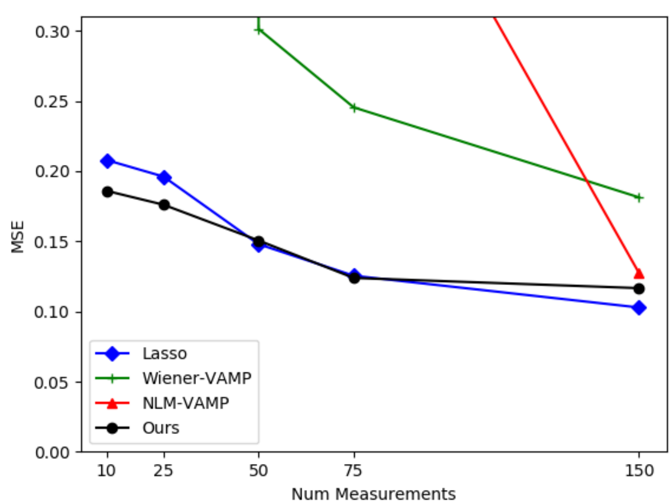

Figure 2. Test loss for recovery from random Gaussian projections on hourly sensor readings of O3 in the air with $n = 1024$ and varying numbers of measurement by our method, Lasso in the DCT basis, NLM-VAMP, and Wiener-VAMP.

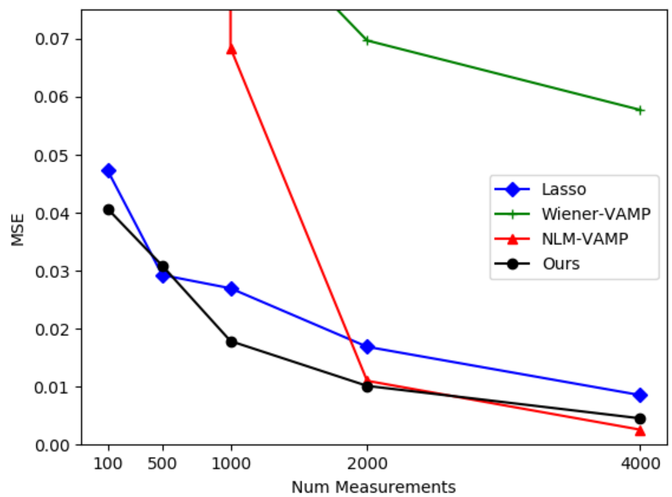

Figure 3. Test loss for recovery from random Gaussian projections on an audio signal of a whale call with $n = 16,384$ and varying numbers of measurement by our method, Lasso in the DCT basis, NLM-VAMP, and Wiener-VAMP.

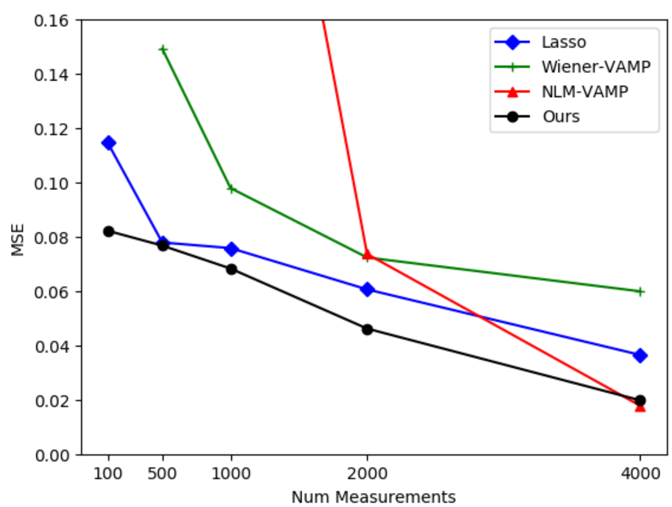

Figure 4. Test loss for recovery from random Gaussian projections on an audio signal of speech with $n = 16,384$ and varying numbers of measurement by our method, Lasso in the DCT basis, NLM-VAMP, and Wiener-VAMP.

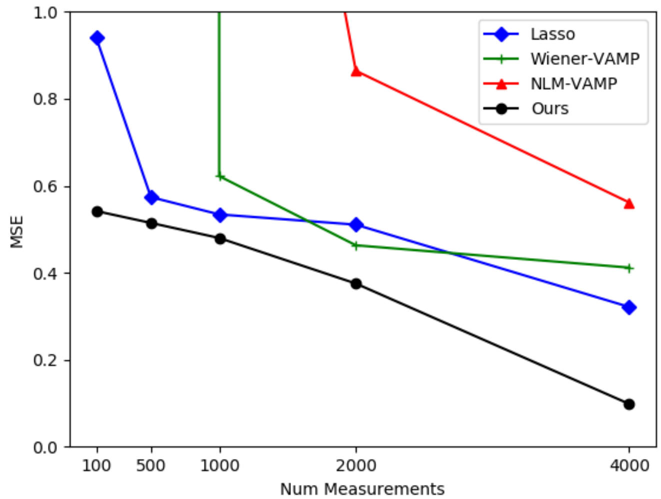

Figure 5. Test loss for recovery from random Gaussian projections on an artificial chirp signal with a 500 hz frequency sweep with $n = 16,384$ and varying numbers of measurement by our method, Lasso in the DCT basis, NLM-VAMP, and Wiener-VAMP.

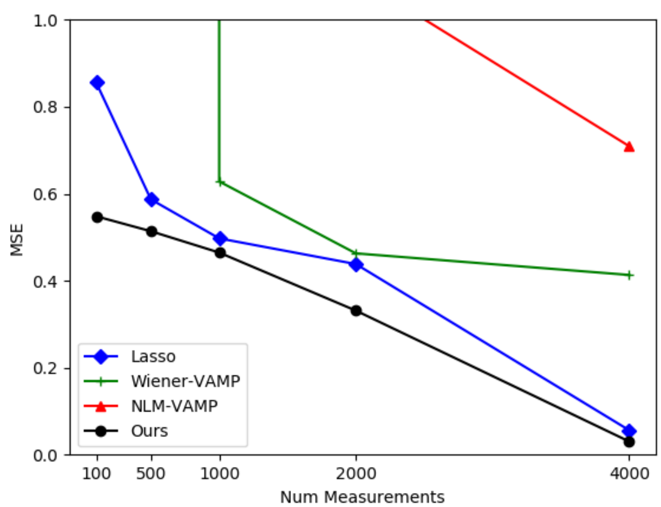

Figure 6. Test loss for recovery from random Gaussian projections on an artificial chirp signal with a 300 hz frequency sweep with $n = 16,384$ and varying numbers of measurement by our method, Lasso in the DCT basis, NLM-VAMP, and Wiener-VAMP.

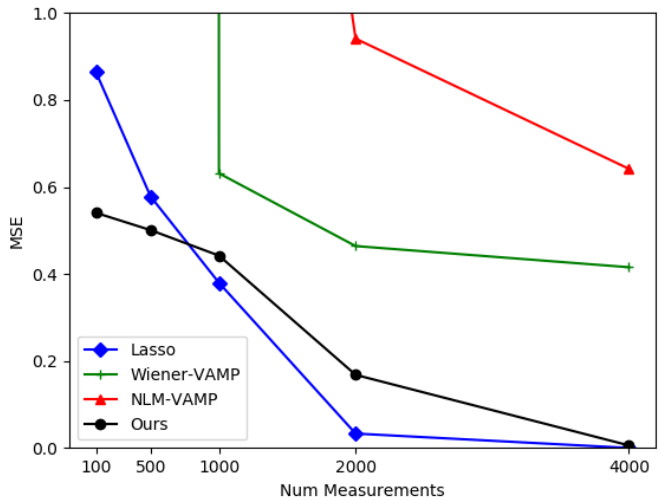

Figure 7. Test loss for recovery from random Gaussian projections on an artificial chirp signal with a 100 hz frequency sweep with $n = 16,384$ and varying numbers of measurement by our method, Lasso in the DCT basis, NLM-VAMP, and Wiener-VAMP.

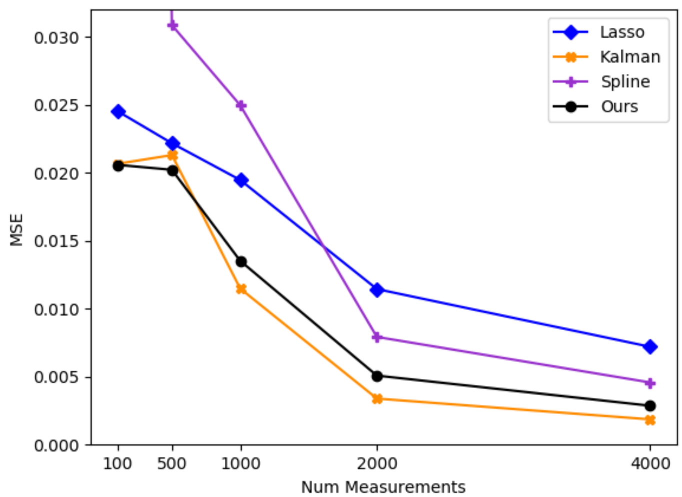

Figure 8. Test loss for imputation on an audio signal of a drum beat with $n = 16,384$ and varying numbers of measurement by our method, Lasso in the DCT basis, Kalman state-space imputation, and spline interpolation.

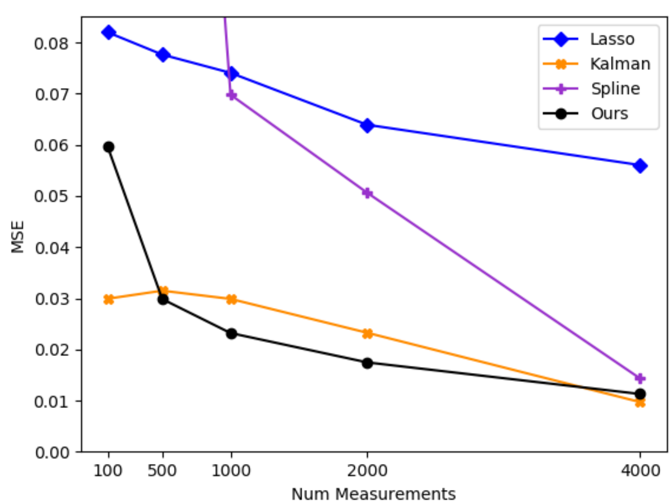

Figure 9. Test loss for imputation on an audio signal of a whale call with $n = 16,384$ and varying numbers of measurement by our method, Lasso in the DCT basis, Kalman state-space imputation, and spline interpolation.

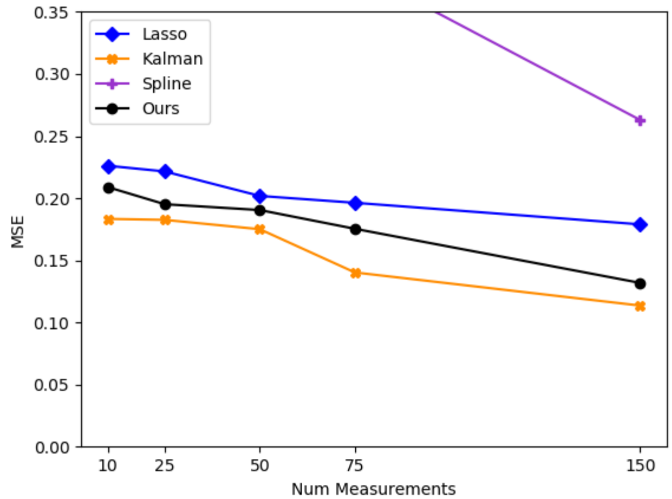

Figure 10. Test loss for imputation on hourly sensor readings of O3 in the air with $n = 1024$ and varying numbers of measurement by our method, Lasso in the DCT basis, Kalman state-space imputation, and spline interpolation.

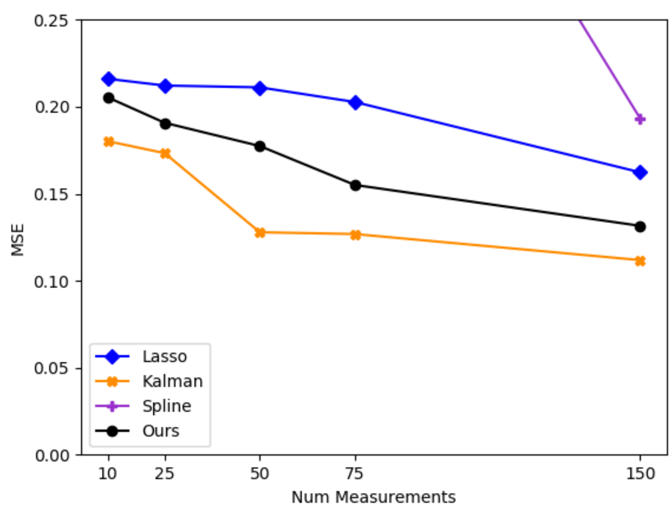

Figure 11. Test loss for imputation on hourly sensor readings of NO2 in the air with $n = 1024$ and varying numbers of measurement by our method, Lasso in the DCT basis, Kalman state-space imputation, and spline interpolation.

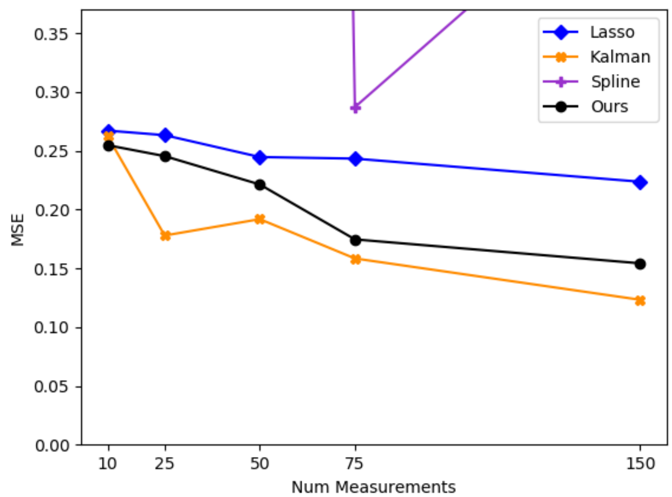

Figure 12. Test loss for imputation on hourly sensor readings of CO in the air with $n = 1024$ and varying numbers of measurement by our method, Lasso in the DCT basis, Kalman state-space imputation, and spline interpolation.

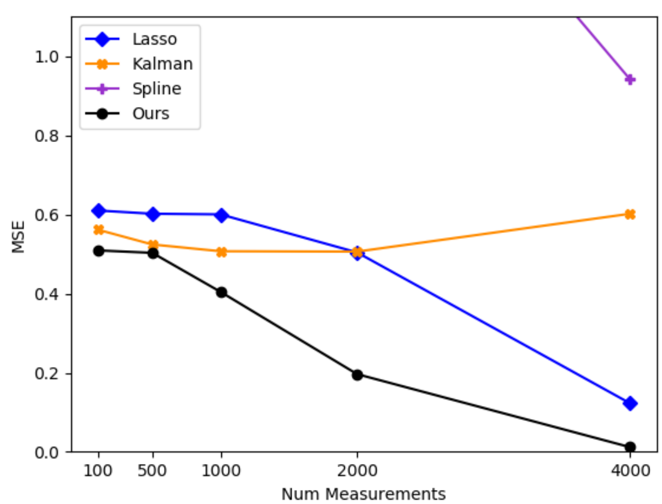

Figure 13. Test loss for imputation on an artificial chirp signal with a 300 hz frequency sweep with $n = 16,384$ and varying numbers of measurement by our method, Lasso in the DCT basis, Kalman state-space imputation, and spline interpolation.

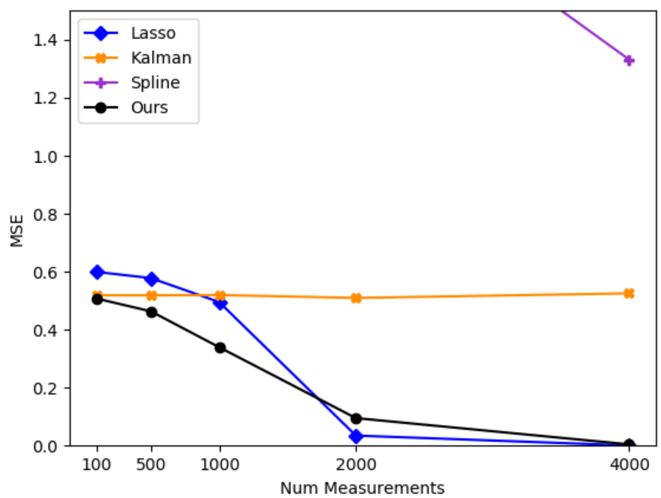

Figure 14. Test loss for imputation on an artificial chirp signal with a 100 hz frequency sweep with $n = 16,384$ and varying numbers of measurement by our method, Lasso in the DCT basis, Kalman state-space imputation, and spline interpolation.